

# LONGITUDINAL SPIN TRANSFER TO THE $\Lambda$ AND $\bar{\Lambda}$ HYPERONS IN MUON-NUCLEON DEEP-INELASTIC SCATTERING

M.G.SAPOZHNIKOV

*for the COMPASS Collaboration*

Joint Institute for Nuclear Research  
Dubna 141980, Russia  
E-mail: sapozh@sunse.jinr.ru

The longitudinal polarization transfer from polarized muons to  $\Lambda$  and  $\bar{\Lambda}$  hyperons has been studied in deep-inelastic scattering at the COMPASS experiment at CERN. The average longitudinal spin transfer to  $\Lambda$  is small:  $S_X(\Lambda) = -0.012 \pm 0.047 \pm 0.024$  at  $\bar{x}_F = 0.22$ . The longitudinal spin transfer to  $\bar{\Lambda}$  is larger:  $S_X(\bar{\Lambda}) = 0.249 \pm 0.056 \pm 0.049$  at  $\bar{x}_F = 0.20$ . The measured  $x$  and  $x_F$  dependences of the longitudinal spin transfer turns out to be different for  $\Lambda$  and  $\bar{\Lambda}$  hyperons. The  $S_X(\Lambda)$  is compatible with zero for all  $x$ , while  $S_X(\bar{\Lambda})$  increases with  $x$  and  $x_F$  and may become as large as  $S_X(\bar{\Lambda}) = 0.4 - 0.5$ .

The study of the  $\Lambda$  and  $\bar{\Lambda}$  hyperon polarization in DIS is important for the understanding of fundamental properties of the nucleon, mechanisms of hyperon production and hyperon spin structure. In particular, it may provide valuable information on the unpolarized strange quark distributions  $s(x)$  and  $\bar{s}(x)$ . Measurements of the spin transfer to hyperons at different polarizations of the target could be used for the determination of the possible polarization of the strange quarks in the nucleon.

We have studied  $\Lambda$  and  $\bar{\Lambda}$  production by scattering of 160 GeV polarized  $\mu^+$  on a polarized  ${}^6\text{LiD}$  target in the framework of COMPASS experiment (NA58) at CERN. A detailed description of the COMPASS experimental setup is given elsewhere [1]. The data used in the present analysis were collected during the years 2003-2004. The event selection requires a reconstructed interaction vertex defined by the incoming and scattered muons and located inside the target, which consists of two 60 cm long, oppositely polarized cells. The data from both longitudinal target spin orientations were recorded simultaneously and averaged in the present analysis. The longitudinally polarized muon

beam has averaged polarization  $P_b = -0.76 \pm 0.04$  in the 2003 run and  $P_b = -0.80 \pm 0.04$  in the 2004 run. The particle identification provided by the ring imaging Cherenkov detector and the calorimeters is not used in the present analysis.

DIS events are selected by cuts on the photon virtuality ( $Q^2 > 1 \text{ (GeV/c)}^2$ ) and on the fractional energy of the virtual photon ( $0.2 < y < 0.9$ ). The events with  $\Lambda$ ,  $\bar{\Lambda}$  and  $K_S^0$  decays are selected by demanding two hadron tracks forming a secondary vertex. The secondary vertex is required to be 5 cm downstream of the target in order to suppress background events. The angle  $\theta_{col}$  between the hyperon momentum and the line joining the primary and secondary vertices should be  $\theta_{col} < 0.01$  rad. A cut on the transverse momentum  $p_t$  of the decay products with respect to the hyperon direction  $p_t > 23 \text{ MeV/c}$  is applied to reject  $e^+e^-$  pairs due to  $\gamma$  conversion. We select events with momenta of positive and negative particles greater than 1 GeV/c. The main sources of background are events from  $K_S^0$  decays and combinatorial background. The percentage of the kaon background changes from 1 to 20 %, when  $\cos\theta_X$  vary from -1 to 1, where  $\theta_X$  is the angle between the direction of the decay proton in the  $\Lambda$  c.m. and the quantization axis. We choose the X-axis along the momentum vector of the virtual photon. In order to minimize the kaon background we limit the angular interval to  $-1 < \cos\theta_X < 0.6$ .

The total statistics after all selection cuts comprises about 70000  $\Lambda$ , 42000  $\bar{\Lambda}$  and 496000  $K_S^0$ .

The distributions for events satisfying the selection cuts on different kinematical variables for  $\Lambda$  and  $\bar{\Lambda}$  are shown in Fig. 1. The shaded histograms show the same distributions for Monte-Carlo events. One can see that the COMPASS Monte Carlo reasonably describes the experimental distributions.

Fig. 1 shows that the COMPASS spectrometer selects  $\Lambda$  in the current fragmentation region. For this analysis we take  $\Lambda(\bar{\Lambda})$  events in the interval  $0.05 < x_F < 0.5$  with the average value  $\bar{x}_F = 0.22(0.20)$ . In contrast with other DIS experiments [2, 3, 4, 5], the COMPASS spectrometer can reach the low  $x$  region with the averaged value  $\bar{x} = 3 \cdot 10^{-2}$ . The averaged  $\Lambda$  fractional energy  $z$  is not large  $\bar{z} = 0.27$ . The averaged values of  $y$  and  $Q^2$  are  $\bar{y} = 0.46$  and  $\bar{Q}^2 = 3.7 \text{ (GeV/c)}^2$ .

The distributions of the kinematic variables for the  $\bar{\Lambda}$  produced in the DIS should be different from the  $\Lambda$  ones, since  $\bar{\Lambda}$  is suppressed in the target fragmentation region. However the acceptance of the COMPASS spectrometer selects the  $\bar{\Lambda}$  with practically the same kinematic distributions as the  $\Lambda$  (see, Fig. 1).

The acceptance corrected angular distribution in the  $\Lambda(\bar{\Lambda})$  rest frame can be written

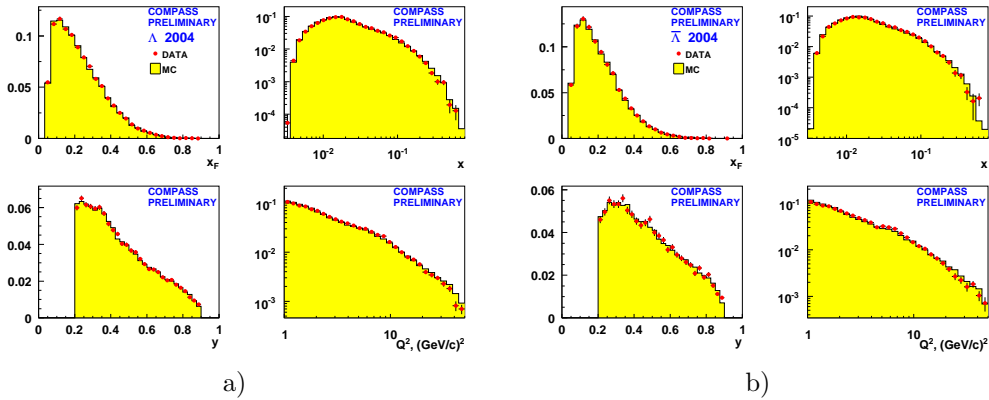


Figure 1: Comparison between the experimental data (circles) and MC (histograms) on  $x_F$ ,  $x$ ,  $y$  and  $Q^2$  distributions of the  $\Lambda$  (a) and  $\bar{\Lambda}$  (b) hyperons. The data are for the 2004 run.

as

$$\frac{1}{N_{tot}^{exp}} \cdot \frac{dN^{exp}}{d \cos \theta_X} = \frac{1}{2} \cdot (1 + \alpha P_X \cos \theta_X). \quad (1)$$

Here  $N_{tot}^{exp}$  is the total number of registered  $\Lambda$  ( $\bar{\Lambda}$ ),  $\alpha = +(-)0.642 \pm 0.013$  is the  $\Lambda$  ( $\bar{\Lambda}$ ) decay parameter,  $P_X$  is the projection of the polarization vector on the X-axis. The acceptance correction was determined using the Monte Carlo simulation for unpolarized  $\Lambda$  and  $\bar{\Lambda}$  decays. To determine the  $\Lambda$  ( $\bar{\Lambda}$ ) angular distributions the sidebands subtraction method is used. The longitudinal polarization  $P_X$  was determined from a fit of the angular distribution (1).

To compare results of different experiments, it is worthwhile to use the longitudinal spin transfer  $S_X$ , which relates the longitudinal polarization of the hyperon  $P_X$  to the polarization of the incoming lepton beam  $P_b$ :  $P_X = S_X \cdot P_b \cdot D(y)$ , where  $D(y)$  is the virtual photon depolarization factor  $D(y) = \frac{1-(1-y)^2}{1+(1-y)^2}$ .

The weighted averaged of the spin transfers for 2003 and 2004 data are:

$$S_X(\Lambda) = -0.012 \pm 0.047 (stat) \pm 0.024 (syst), \quad (2)$$

$$S_X(\bar{\Lambda}) = 0.249 \pm 0.056 (stat) \pm 0.049 (syst). \quad (3)$$

The main sources of systematics errors are the uncertainty of the MC simulation of  $\pm 0.016$  ( $\pm 0.016$ ) and variation of the selection cuts  $\pm 0.016$  ( $\pm 0.044$ ) for  $\Lambda$  ( $\bar{\Lambda}$ ) spin

transfer, correspondingly. Another source of systematic errors is the uncertainty in the beam polarization, which amounts to 5.3%. The uncertainty of the sidebands subtraction method was found to be  $\pm 0.010$  ( $\pm 0.016$ ).

The  $x$  and  $x_F$  dependences of the spin transfers to  $\Lambda$  and  $\bar{\Lambda}$  are shown in Fig. 2. The

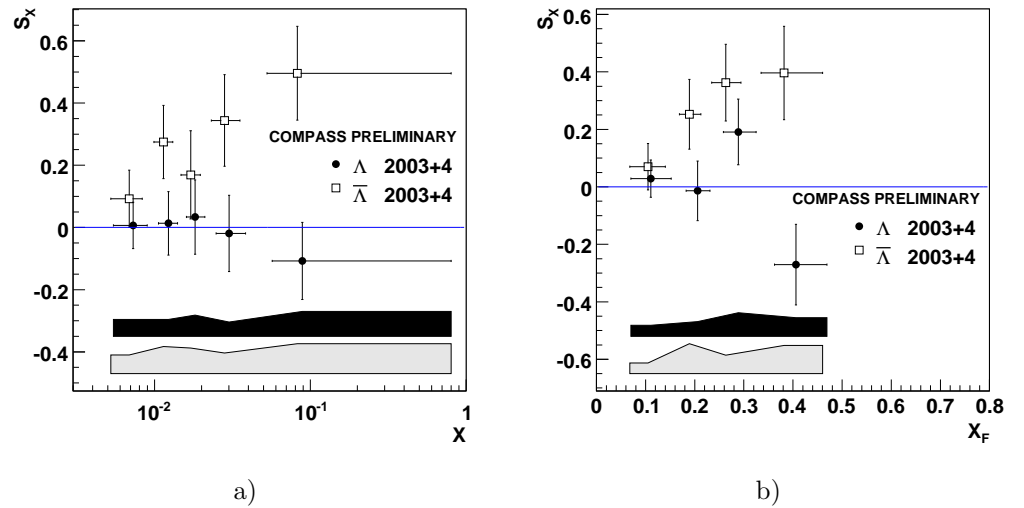


Figure 2: The  $x$ - (a) and  $x_F$  (b) dependences of the longitudinal spin transfer to  $\Lambda$  and  $\bar{\Lambda}$ . The shaded bands show the size of the corresponding systematic errors.

$x$ -dependence of the spin transfer demonstrates the difference in the longitudinal spin transfer for  $\Lambda$  and  $\bar{\Lambda}$ . The spin transfer to  $\Lambda$  is small. In all  $x$ -interval it is compatible with zero. The spin transfer to  $\bar{\Lambda}$  is non-zero and increases at  $x \sim (5 - 10) \cdot 10^{-2}$ . A similar difference between  $\Lambda$  and  $\bar{\Lambda}$  spin transfer is observed in the  $x_F$  dependence of Fig. 2 (b). The spin transfer to  $\bar{\Lambda}$  increases with  $x_F$ . The  $x_F$  and  $x$  dependences show that the longitudinal spin transfer to  $\bar{\Lambda}$  may reach values as large as  $S_X(\bar{\Lambda}) = 0.4 - 0.5$ .

The  $x_F$  dependence of the spin transfer to  $\Lambda$  and  $\bar{\Lambda}$  for COMPASS and other experiments is shown in Fig. 3. The measurement of E665 Collaboration [4] indicates on the positive spin transfer for  $\bar{\Lambda}$  (see Fig. 3). Our results confirm this observation but on much more better statistical level. The NOMAD collaboration [2] obtain for the current fragmentation region ( $x_F > 0$ )  $S_X(\Lambda) = 0.09 \pm 0.06 \pm 0.03$  at  $\bar{x}_F = 0.21$ , which is compatible with our value  $S_X(\Lambda) = -0.012 \pm 0.047 \pm 0.024$  at  $\bar{x}_F = 0.22$ , indicating a small spin transfer to  $\Lambda$ . The NOMAD collaboration has also found [3]

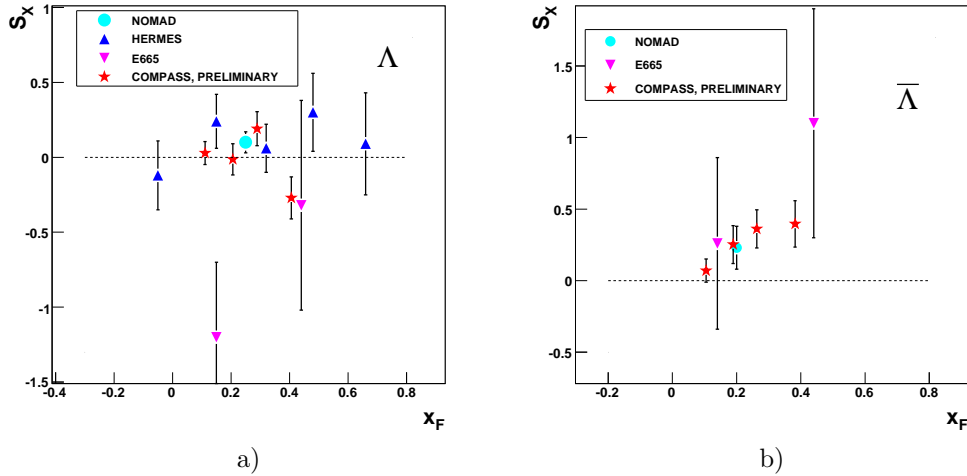


Figure 3: The  $x_F$  dependence of the longitudinal spin transfer to  $\Lambda$  (a) and  $\bar{\Lambda}$  (b) for the COMPASS (stars) and other experiments [2, 3, 4, 5] (NOMAD data- circles, E665 - reverse triangles, HERMES - triangles).

that the spin transfer to  $\bar{\Lambda}$  is  $S_X(\bar{\Lambda})=0.23 \pm 0.15 \pm 0.08$  at  $\bar{x}_F = 0.18$ . Our result  $S_X(\bar{\Lambda})=0.249 \pm 0.056 \pm 0.049$  at  $\bar{x}_F = 0.20$  is in a good agreement with their value. The results of the HERMES Collaboration [5] are shown in Fig. 3. The average value of the spin transfer  $S_X(\Lambda)=0.11 \pm 0.10 \pm 0.03$  at  $\langle z \rangle = 0.45$  is in agreement with (2).

The main conclusion from the results of (2)-(3) is that the longitudinal spin transfers to  $\Lambda$  and  $\bar{\Lambda}$  hyperons in DIS are not equal. That is a non-trivial observation, especially if one take note on the practically similar  $x_F$  and  $x$ -distributions of  $\Lambda$  and  $\bar{\Lambda}$  shown in Fig.1. That indicates that the production mechanisms of  $\Lambda$  and  $\bar{\Lambda}$  are the same, but the spin transfer dynamics is different. Earlier theoretical calculations of  $\Lambda$  and  $\bar{\Lambda}$  polarization at the COMPASS energy [6] indeed predicted practically equal values for  $P(\Lambda)$  and  $P(\bar{\Lambda})$ . Recent calculation of [7] shows that at the COMPASS energy the spin transfer to  $\bar{\Lambda}$  must be larger than to  $\Lambda$ . It shows also that the spin transfer to  $\bar{\Lambda}$  in DIS strongly depends on the antistrange quark distribution. To demonstrate the degree of the sensitivity to the strange quark distributions, in Fig. 4 the data of the spin transfer to  $\bar{\Lambda}$  is compared with results of calculations [7] for the CTEQ5L [8](solid lines) and the GRV98LO [9](dashed lines) sets of parton distribution functions. The GRV98 set is

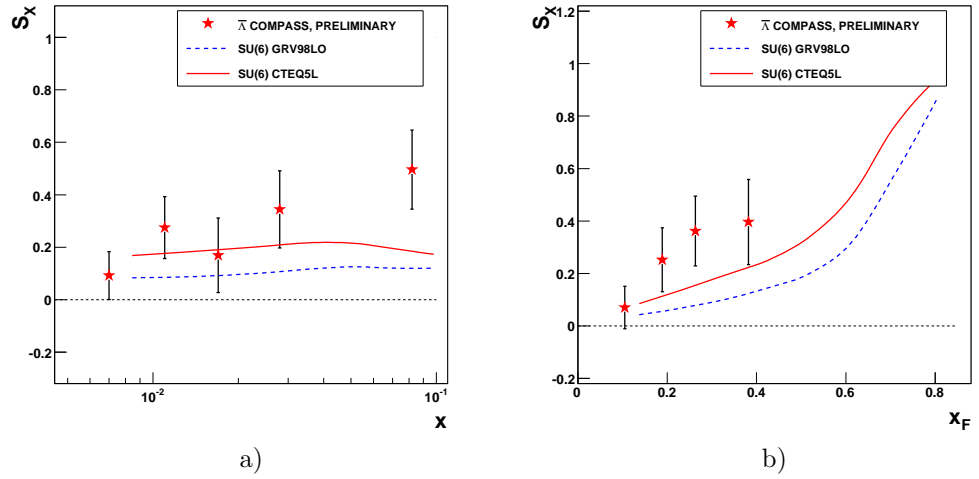


Figure 4: The  $x$  (a) and  $x_F$  (b) dependences of the longitudinal spin transfer to  $\bar{\Lambda}$  calculated in [7] (Model B, SU(6)) for two sets of the parton distribution functions: GRV98LO (dashed lines) and CTEQ5L (solid lines).

chosen because of its assumption that there is no intrinsic nucleon strangeness at a low scale and the strange sea is of pure perturbative origin. The CTEQ collaboration allows non-perturbative strangeness in the nucleon. The amount of this intrinsic strangeness is fixed from the dimuon data of the CCFR and NuTeV experiments [10, 11]. As a result, the  $s(x)$  distribution of CTEQ is larger than the GRV98 one by a factor of about two in the region  $x = 0.001 - 0.01$ . The results in Fig. 4 show how the spin transfer to the  $\bar{\Lambda}$  reflects this difference in the  $s$  quark distributions. The CTEQ parton distribution results in larger spin transfer to both  $x$ - and  $x_F$ -dependences and better agree with our data than the GRV98 ones.

Therefore, precise measurements of the  $\bar{\Lambda}$  spin transfer could give useful information about the anti-strange quark distribution, which could be complementary to the inclusive electroproduction deep-inelastic data, which are sensitive to the sum  $s(x) + \bar{s}(x)$  of unpolarized distributions.

The COMPASS data presented here are the most precise measurements to date of the longitudinal spin transfer to  $\Lambda$  and  $\bar{\Lambda}$  in deep-inelastic scattering.

**References**

- [1] COMPASS, P.Abbon *et al.*, Nucl.Instr.Meth. **A577** (2007) 455.
- [2] NOMAD, P.Astier *et al.*, Nucl.Phys. **B588** (2000) 3.
- [3] NOMAD, P.Astier *et al.*, Nucl.Phys. **B605** (2001) 3.
- [4] E665, M.R.Adams *et al.*, Eur.Phys.J. **C17** (2000) 263.
- [5] HERMES, A.Airapetian *et al.*, Phys.Rev. **D74** (2006) 072004. [6]
- [6] Dong Hui, Zhou Jian and Liang Zuo-tang, Phys.Rev.**D72** (2005) 033006
- [7] J. Ellis, A.M. Kotzinian, D. Naumov and M.G. Sapozhnikov, Eur.Phys.J. **C52** (2007) 283
- [8] CTEQ, F.Olness *et al.*, Eur.Phys.J. **C40** (2005) 145.
- [9] M. Gluck, E. Reya and A. Vogt, Eur. Phys. J. **C5** (1998) 461.
- [10] CCFR, M.Goncharov *et al.*, Phys.Rev. **D64** (2001) 112006.
- [11] NuTeV, M.Tzanov *et al.*, hep-ex/0306035, (2003)